2008-01-1160

How to Play a Disc Brake: A Dissipation-Induced Squeal

Oleg N. Kirillov
Technische Universität Darmstadt
Institute of Mechanics, Moscow State Lomonosov University

ABSTRACT

The eigenvalues of an elastic body of revolution, rotating about its axis of symmetry, form a 'spectral mesh'. The nodes of the mesh in the plane 'frequency' versus 'gyroscopic parameter' correspond to the double eigenfrequencies. With the use of the perturbation theory of multiple eigenvalues, deformation of the spectral mesh caused by dissipative and non-conservative perturbations, originating from the frictional contact, is analytically described. The key role of indefinite damping and non-conservative positional forces in the development of the subcritical flutter instability is clarified. A clear mathematical description is given for the mechanism of excitation of particular modes of rotating structures in frictional contact, such as squealing disc brakes and singing wine glasses.

INTRODUCTION

An axially symmetric shell, like a wine glass, can easily produce sound when a wet finger is rubbed around its rim or wall, as it was observed already in 1638 by Galileo Galilei in his Dialogues Concerning Two New Sciences [6, 29]. This principle is used in playing the glass harmonica invented by Benjamin Franklin in 1761, which he called 'armonica', where, in order to produce sound, one should touch by a moist finger an edge of a glass bowl rotating about its axis of symmetry [12, 19, 29, 47]. This remarkable phenomenon has been studied experimentally; see e.g. [35]. However, an adequate theory for its description seems to be still missing. Another closely related example of acoustics of friction is the squealing disc brake [19, 23, 34]. This mechanical system produces sound due to transverse vibrations of a rotating annular plate caused by its interaction with the brake pads. Despite intensive experimental and theoretical study, the problem of predicting and controlling the squeal remains an important issue [10, 16, 19, 21, 23, 34, 42, 43, 48, 49]. Significant but still poorly understood phenomena are squealing and barring of calender rolls in paper mills causing a noise and reducing the quality of the paper [30].

The presence of multiple eigenvalues in the spectra of free vibrations of axially symmetric shells and plates is well known. Already Rayleigh, studying the acoustics of bells, recognized that, if the symmetry of a bell were complete, the nodal meridians of a transverse vibration mode would have no fixed position but would travel freely around the bell, as do those in a wine glass driven by the moistened finger [19]. This is a reflection of the fact that spectra of free vibrations of a bell, a wine glass, an annular plate, and other bodies of revolution contain double purely imaginary semi-simple eigenvalues with two linearly independent eigenvectors.

Rotation causes the double eigenvalues of an axially symmetric structure to split [1]. The newborn pair of simple eigenvalues corresponds to the forward and backward traveling waves, which propagate along the circumferential direction [1, 2, 3, 7, 13, 16, 17]. Viewed from the rotational frame, the frequency of the forward traveling wave appears to decrease and that of the backward traveling wave appears to increase, as the spin increases. Due to this fact, double eigenvalues originate again at non-zero angular velocities, forming the nodes of the spectral mesh in the plane 'eigenfrequency' versus 'angular velocity'. The spectral meshes are characteristic for the rotating circular strings, rings, discs, and cylindrical and hemispherical shells. The phenomenon is apparent also in hydrodynamics, in the problem of stability of a vortex tube [24] and in magnetohydrodynamics in the problem of instability of the spherically symmetric MHD α^2-dynamo [38].

It is known that striking the wine glass excites a number of modes, but rubbing the rim with a finger generally excites a single mode [12]. Similar phenomenon is observed for the squealing disc brake [19, 23, 34, 39, 40, 41]. For this reason, we formulate the main problem of acoustics of friction of rotating elastic bodies of revolution as the description of the mechanism of activating a particular mode of the continuum by its contact with an external body.

In case of the disc brake, the frictional contact of the brake pads with the rotating disc introduces dissipative and non-conservative positional forces into the system [34, 43, 46, 48]. Since the nodes of the spectral mesh correspond to the double eigenvalues, they are most sensitive to perturbations, especially to those breaking

the symmetries of the system. Consequently, the instability will most likely occur at the angular velocities close to that of the nodes of the spectral mesh. The unstable modes of the perturbed system will have the frequencies close to that of the double eigenvalues at the nodes. This picture qualitatively agrees with the existing experimental data [12, 19, 23, 34, 39, 40, 41].

In the following using the perturbation theory of multiple eigenvalues [28, 32, 33, 38] we will show that independently on the definiteness of the damping matrix, there exist combinations of dissipative and non-conservative positional forces, causing the flutter instability in the vicinity of the nodes of the spectral mesh for the angular velocities from the subcritical range. Zero and negative eigenvalues in the spectrum of the damping matrix encourage the development of the localized subcritical flutter instability while zero eigenvalues in the matrix of non-conservative positional forces suppress it. Explicit expressions describing the movements of eigenvalues due to change of the system parameters will be obtained. Conditions will be derived for the eigenvalues to move to the right part of the complex plane. Approximations of the domain of asymptotic stability will be found and singularities of the stability boundary responsible for the development of instability will be described and classified. The methodology developed for the study of the two-dimensional system will finally be employed to the detailed investigation of the stability of a rotating circular string constrained by a stationary load system.

THE SPECTRAL MESH OF A GYROSCOPIC SYSTEM WITH TWO DEGREES OF FREEDOM

Consider an autonomous non-conservative system

$$\text{(1)}\quad \ddot{\mathbf{x}} + (2\Omega\mathbf{G} + \delta\mathbf{D})\dot{\mathbf{x}} + ((\beta^2 - \Omega^2)\mathbf{I} + \kappa\mathbf{K} + \nu\mathbf{N})\mathbf{x} = 0,$$

where a dot over a symbol denotes time differentiation, $\mathbf{x} \in R^2$, and $\mathbf{I}$ is the identity matrix. The real matrices $\mathbf{D} = \mathbf{D}^T$, $\mathbf{G} = -\mathbf{G}^T$, $\mathbf{K} = \mathbf{K}^T$, and $\mathbf{N} = -\mathbf{N}^T$ are related to dissipative (damping), gyroscopic, potential, and non-conservative positional (circulatory) forces with magnitudes controlled by scaling factors δ, Ω, κ, and ν respectively; $\beta > 0$ is the frequency of free vibrations of the potential system, corresponding to $\delta = \Omega = \kappa = \nu = 0$. The parameters and variables of the system are assumed to be non-dimensional quantities. Without loss in generality it is accepted that $\det\mathbf{G} = 1$ and $\det\mathbf{N} = 1$. Equation (1) frequently appears as a two-mode approximation of the models of rotating elastic bodies of revolution in frictional contact after their linearization and discretization [16, 23, 46].

Separating time by setting $\mathbf{x}(t) = \mathbf{u}\exp(\lambda t)$ we arrive at the eigenvalue problem $\mathbf{L}\mathbf{u} = 0$, where

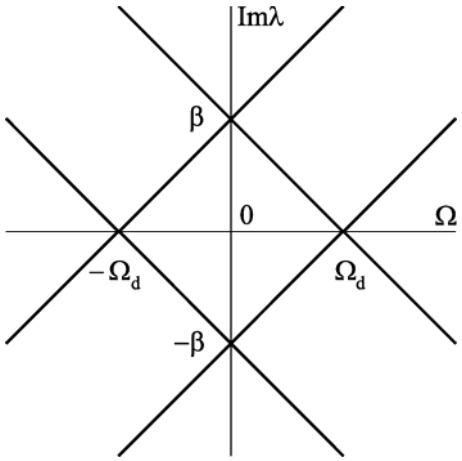

Figure 1.
The spectral mesh of system (1) when $\delta = \kappa = \nu = 0$.

$$\text{(2)}\quad \mathbf{L} = \mathbf{I}\lambda^2 + (2\Omega\mathbf{G} + \delta\mathbf{D})\lambda + (\beta^2 - \Omega^2)\mathbf{I} + \kappa\mathbf{K} + \nu\mathbf{N}$$

Applying the Leverrier-Barnett algorithm [9] to the operator $\mathbf{L}$ we find the characteristic polynomial

$$\begin{aligned}\text{(3)}\quad & P(\lambda) = \lambda^4 + \delta\mathrm{Tr}\mathbf{D}\lambda^3 \\ & + (2(\beta^2 + \Omega^2) + \delta^2\det\mathbf{D} + \kappa\mathrm{Tr}\mathbf{K})\lambda^2 \\ & + (4\Omega\nu + \delta(\beta^2 - \Omega^2)\mathrm{Tr}\mathbf{D} + \delta\kappa(\mathrm{Tr}\mathbf{K}\mathrm{Tr}\mathbf{D} - \mathrm{Tr}\mathbf{K}\mathbf{D}))\lambda \\ & + \kappa^2\det\mathbf{K} + \kappa\mathrm{Tr}\mathbf{K}(\beta^2 - \Omega^2) + (\beta^2 - \Omega^2)^2 + \nu^2,\end{aligned}$$

where Tr stands for the trace of a matrix. In the absence of dissipative, external potential, and non-conservative positional forces the polynomial (3), corresponding to the operator $\mathbf{L}_0(\Omega) = \mathbf{I}\lambda^2 + 2\lambda\Omega\mathbf{G} + (\beta^2 - \Omega^2)\mathbf{I}$, has four purely imaginary roots [18]

$$\text{(4)}\quad \lambda_p^{\pm} = i\beta \pm i\Omega, \quad \lambda_n^{\pm} = -i\beta \pm i\Omega$$

In the plane $(\Omega, \mathrm{Im}\,\lambda)$ equations (4) describe straight lines intersecting with each other (Fig. 1) - *the spectral mesh* [38]. Two nodes of the mesh at $\Omega = 0$ correspond to the double semi-simple eigenvalues $\lambda = \pm i\beta$. At the other two nodes at $\Omega = \pm\Omega_d$ there exist double semi-simple eigenvalues $\lambda = 0$. The range $|\Omega| < \Omega_d = \beta$ is called *subcritical* for the gyroscopic parameter Ω [18]. The double semi-simple eigenvalue $i\beta$ at $\Omega = \Omega_0 = 0$ has two linearly-independent eigenvectors $\mathbf{u}_1$ and $\mathbf{u}_2$

$$\text{(5)}\quad \mathbf{u}_1 = \frac{1}{\sqrt{2\beta}}\begin{pmatrix}0\\1\end{pmatrix}, \quad \mathbf{u}_2 = \frac{1}{\sqrt{2\beta}}\begin{pmatrix}1\\0\end{pmatrix}.$$

The eigenvectors are orthogonal $\mathbf{u}_i^T\mathbf{u}_j = 0$, $i \neq j$, and satisfy the normalization condition $\mathbf{u}_i^T\mathbf{u}_i = (2\beta)^{-1}$.

Under variation of the gyroscopic parameter $\Omega = \Omega_0 + \Delta\Omega$, the double eigenvalue $i\beta$ into two simple ones bifurcates. The asymptotic formula for the perturbed eigenvalues is [32]

$$(6)\ \lambda_p^{\pm} = i\beta + i\Delta\Omega\frac{f_{11}+f_{22}}{2} \pm i\Delta\Omega\sqrt{\frac{(f_{11}-f_{22})^2}{4}+f_{12}f_{21}}$$

where the quantities f_{ij} are

$$(7)\ f_{ij} = \mathbf{u}_j^T \frac{\partial \mathbf{L}_0(\Omega)}{\partial\Omega}\mathbf{u}_i\bigg|_{\Omega=0,\lambda=i\beta} = 2i\beta\mathbf{u}_j^T\mathbf{G}\mathbf{u}_i .$$

The skew symmetry of $\mathbf{G}$ yields $f_{11} = f_{22} = 0$, $f_{12} = -f_{21} = i$, so that (6) gives the exact result (4).

DEFORMATION OF THE SPECTRAL MESH

Consider a perturbation of the gyroscopic system $\mathbf{L}_0(\Omega) + \Delta\mathbf{L}(\Omega)$, assuming that the size of the perturbation $\Delta\mathbf{L}(\Omega) = \delta\lambda\,\mathbf{D} + \kappa\,\mathbf{K} + \nu\,\mathbf{N} \sim \varepsilon$ is small, where $\varepsilon = \|\Delta\mathbf{L}(0)\|$. The behavior of the perturbed double eigenvalue $i\beta$ for small Ω and ε is described by the asymptotic formula [32]

$$(8)\ \lambda = i\beta + i\Omega\frac{f_{11}+f_{22}}{2} + i\frac{\xi_{11}+\xi_{22}}{2} \pm i\sqrt{\frac{(\Omega(f_{11}-f_{22})+\xi_{11}-\xi_{22})^2}{4}+(\Omega f_{12}+\xi_{12})(\Omega f_{21}+\xi_{21})}$$

where f_{ij} are given by (7) and

$$(9)\ \xi_{ij} = \mathbf{u}_j^T\Delta\mathbf{L}(0)\mathbf{u}_i = i\beta\delta\mathbf{u}_j^T\mathbf{D}\mathbf{u}_i + \kappa\mathbf{u}_j^T\mathbf{K}\mathbf{u}_i + \nu\mathbf{u}_j^T\mathbf{N}\mathbf{u}_i$$

are small complex numbers of order ε. With the vectors (5) we obtain

$$(10)\ \lambda = i\beta + i\frac{\rho_1+\rho_2}{4\beta}\kappa - \frac{\mu_1+\mu_2}{4}\delta \pm \sqrt{c},$$

$$(11)\ c = \left(\frac{\mu_1-\mu_2}{4}\right)^2\delta^2 - \left(\frac{\rho_1-\rho_2}{4\beta}\right)^2\kappa^2 + \left(i\Omega+\frac{\nu}{2\beta}\right)^2 - i\delta\kappa\frac{2\mathrm{Tr}\mathbf{K}\mathbf{D}-\mathrm{Tr}\mathbf{K}\mathrm{Tr}\mathbf{D}}{8\beta},$$

where μ_1, μ_2 and ρ_1, ρ_2 are eigenvalues of $\mathbf{D}$ and $\mathbf{K}$, respectively, and thus satisfy the equations

$$(12)\ \mu^2 - \mu\mathrm{Tr}\mathbf{D} + \det\mathbf{D} = 0, \quad \rho^2 - \rho\mathrm{Tr}\mathbf{K} + \det\mathbf{K} = 0.$$

Separation of real and imaginary parts in (10) yields

$$(13)\ \mathrm{Re}\,\lambda = -\frac{\mu_1+\mu_2}{4}\delta \pm \sqrt{\frac{\mathrm{Re}\,c + \sqrt{(\mathrm{Re}\,c)^2+(\mathrm{Im}\,c)^2}}{2}},$$

$$\mathrm{Im}\,\lambda = \beta + \frac{\rho_1+\rho_2}{4\beta}\kappa \pm \sqrt{\frac{-\mathrm{Re}\,c + \sqrt{(\mathrm{Re}\,c)^2+(\mathrm{Im}\,c)^2}}{2}},$$

where

$$(14)\ \mathrm{Im}\,c = \frac{\Omega\nu}{\beta} - \delta\kappa\frac{2\mathrm{Tr}\mathbf{K}\mathbf{D}-\mathrm{Tr}\mathbf{K}\mathrm{Tr}\mathbf{D}}{8\beta}$$

$$\mathrm{Re}\,c = \left(\frac{\mu_1-\mu_2}{4}\right)^2\delta^2 - \left(\frac{\rho_1-\rho_2}{4\beta}\right)^2\kappa^2 - \Omega^2 + \frac{\nu^2}{4\beta^2}.$$

The formulas (10) – (14) describe splitting of the double eigenvalues at the nodes of the spectral mesh due to variation of parameters, including those corresponding to dissipative and non-conservative positional forces. This leads to the deformation of the mesh, in particular, to the *veering* and *merging* of eigenvalue branches.

Although the veering phenomenon in the systems with gyroscopic coupling was studied both numerically and analytically, e.g in [3, 4, 7, 8, 13, 17, 31], the explicit expressions (10) - (14) for the splitting of the double eigenvalues due to action of forces of all types were not previously derived. The approach used in our paper is distinct of that of the cited works. It is based on the perturbation theory of multiple eigenvalues [28, 32, 33]. The spectrum of the perturbed system is described by means of only the derivatives of the operator with respect to parameters and the eigenvectors of the multiple eigenvalue calculated directly at a node of the spectral mesh.

THE EFFECT OF POTENTIAL FORCES

We first study the influence of a conservative perturbation with the matrix $\mathbf{K}$ on the spectral mesh of the gyroscopic system. Substituting $\delta = \nu = 0$ into the formulas (13) and (14) and transforming them yields

$$(15)\ \left(\mathrm{Im}\,\lambda - \beta - \frac{\rho_1+\rho_2}{4\beta}\right)^2 - \Omega^2 = \left(\frac{\rho_1-\rho_2}{4\beta}\right)^2\kappa^2,$$

$$\mathrm{Re}\,\lambda = 0.$$

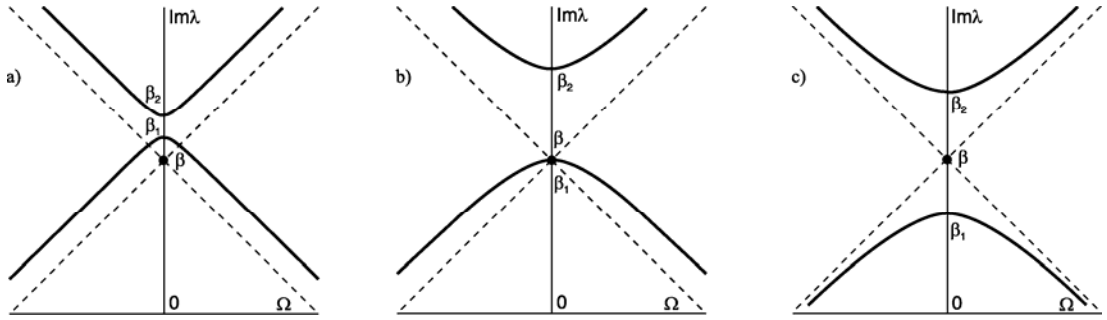

Figure 2.

Conservative deformation of the spectral mesh ($\kappa > 0$): $\mathbf{K} > 0$ (a); $\mathbf{K}$ is positive semi-definite (b); $\mathbf{K}$ is indefinite (c).

When $\kappa \neq 0$, equation (15) describes a hyperbola in the plane $\mathrm{Im}\,\lambda$ versus Ω with the asymptotes

$$\text{(16)}\quad \mathrm{Im}\,\lambda = \beta + \frac{\rho_1 + \rho_2}{4\beta}\kappa \pm \Omega.$$

The asymptotes cross each other above the node $(0, \beta)$ of the non-deformed spectral mesh for $\mathrm{Tr}\mathbf{K} > 0$, exactly at the node for $\rho_1 = -\rho_2$, and below the node for $\mathrm{Tr}\mathbf{K} < 0$. The branches of the hyperbola intersect the axis $\Omega = 0$ at the points

$$\text{(17)}\quad \beta_1 = \beta + \frac{\rho_1}{2\beta}\kappa, \quad \beta_2 = \beta + \frac{\rho_2}{2\beta}\kappa.$$

If the eigenvalues $\rho_{1,2}$ have the same sign, the intersection points are always located above or below the node of the spectral mesh for $\mathbf{K} > 0$ or $\mathbf{K} < 0$, respectively, see Fig. 2(a). In case when one of the eigenvalues $\rho_{1,2}$ is zero, implying semi-definiteness of the matrix $\mathbf{K}$, one of the branches of the hyperbola goes through the node of the spectral mesh and the other crosses the axis $\Omega = 0$ above the node, if $\mathbf{K}$ is positive semi-definite, or below it, if $\mathbf{K}$ is negative semi-definite, Fig. 2(b). If $\mathbf{K}$ is indefinite, one of the intersection points $\beta_{1,2}$ is located above the node and another one below the node, as indicated in Fig. 2(c).

Therefore, the conservative deformation of the spectral mesh does not shift the eigenvalues from the imaginary axis, preserving the marginal stability. However, the deformation pattern depends on the definiteness of the perturbation matrix $\mathbf{K}$. In particular, in the degenerate case when $\det\mathbf{K} = 0$, one of the eigenvalue branches, originated after the splitting of the double eigenvalue, always passes through the point corresponding to the node of the unperturbed spectral mesh, Fig. 2(b).

CREATION AND ACTIVATION OF THE LATENT SOURCES OF INSTABILITY BY DISSIPATION

Consider the effect of dissipative forces on the stability of the gyroscopic system and study its dependence on the properties of the matrix $\mathbf{D}$. Assuming $\nu = \kappa = 0$ in expression (11) we rewrite formula (10) in the form

$$\text{(18)}\quad \lambda = i\beta - \frac{\mu_1 + \mu_2}{4}\delta \pm \sqrt{\left(\frac{\mu_1 - \mu_2}{4}\right)^2 \delta^2 - \Omega^2}.$$

Since $\mathrm{Im}\,c = 0$, equations (13) are transformed into

$$\text{(19)}\quad \left(\mathrm{Re}\,\lambda + \frac{\mu_1 + \mu_2}{4}\delta\right)^2 + \Omega^2 = \frac{(\mu_1 - \mu_2)^2}{16}\delta^2, \qquad \mathrm{Im}\,\lambda = \beta$$

when

$$\text{(20)}\quad \Omega^2 - \frac{(\mu_1 - \mu_2)^2}{16}\delta^2 < 0,$$

and into

$$\text{(21)}\quad \Omega^2 - (\mathrm{Im}\,\lambda - \beta)^2 = \frac{(\mu_1 - \mu_2)^2}{16}\delta^2, \qquad \mathrm{Re}\,\lambda = -\frac{\mu_1 + \mu_2}{4}\delta,$$

for the opposite sign in inequality (20) . For a given δ equation (21) defines a hyperbola in the plane $(\Omega, \mathrm{Im}\,\lambda)$, while (19) is the equation of a circle in the plane $(\Omega, \mathrm{Re}\,\lambda)$, as shown in Fig. 3(a,c). For tracking the complex eigenvalues due to change of Ω, it is convenient to consider the eigenvalue branches in the three-dimensional space $(\Omega, \mathrm{Im}\,\lambda, \mathrm{Re}\,\lambda)$.

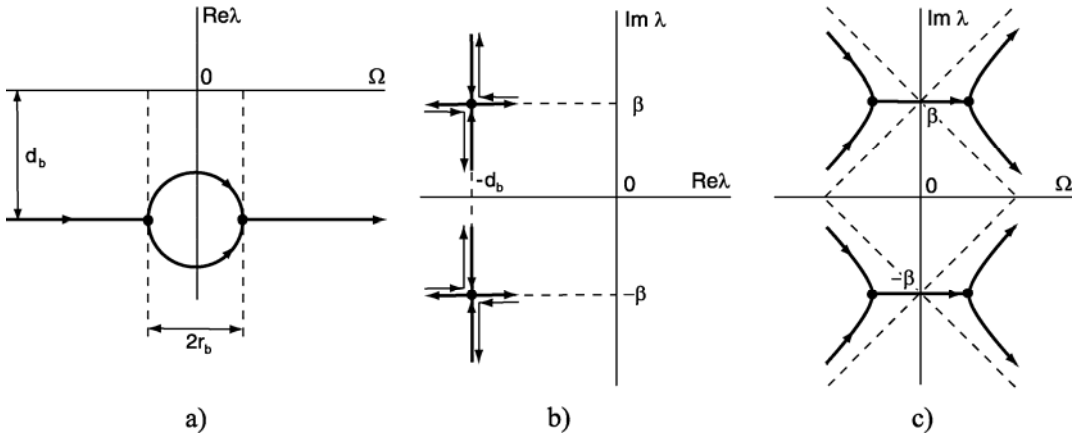

Figure 3. Origination of a latent source of the subcritical flutter instability in presence of full dissipation.

In this space the circle belongs to the plane $\mathrm{Im}\,\lambda = \beta$ and the hyperbola lies in the plane $\mathrm{Re}\,\lambda = -\delta(\mu_1 + \mu_2)/4$, see Fig. 4(a,c).

Below we show that the circle of the complex eigenvalues - *the bubble of instability* [20] - plays the crucial role in the development and localization of the subcritical flutter instability. Its properties depend on whether the matrix $\mathbf{D}$ is definite or indefinite.

Full dissipation and pervasive damping: A latent state of the bubble of instability

Formulas (19) and (21) show that the radius of the bubble of instability r_b and the distance d_b of its center from the plane $\mathrm{Re}\,\lambda = 0$ are defined by the eigenvalues μ_1 and μ_2 of the matrix $\mathbf{D}$

$$(22)\quad r_b = \frac{|(\mu_1 - \mu_2)\delta|}{4}, \quad d_b = \frac{|(\mu_1 + \mu_2)\delta|}{4}.$$

Consequently, the bubble of instability is "submerged" under the surface $\mathrm{Re}\,\lambda = 0$ in the space $(\Omega, \mathrm{Im}\,\lambda, \mathrm{Re}\,\lambda)$. It does not intersect the plane $\mathrm{Re}\,\lambda = 0$ under the conditions

$$(23)\quad \delta(\mu_1 + \mu_2) = \delta\,\mathrm{tr}\mathbf{D} > 0,\ \mu_1\mu_2 = \det\mathbf{D} \geq 0,$$

where the latter is equivalent to the inequality $d_b \geq r_b$. The inequalities (23) imply positive semi-definiteness of the matrix $\delta\mathbf{D}$. Hence, the role of full dissipation or pervasive damping is to deform the spectral mesh in such a way that the double eigenvalue is inflated to the bubble of complex eigenvalues (19) connected with the two branches of the hyperbola (21) at the points

$$(24)\quad \begin{aligned} &\mathrm{Im}\,\lambda = \beta, \quad \mathrm{Re}\,\lambda = -\delta(\mu_1 + \mu_2)/4, \\ &\Omega = \pm\delta(\mu_1 - \mu_2)/4, \end{aligned}$$

and to plunge all the eigenvalue curves into the region $\mathrm{Re}\,\lambda \leq 0$. The eigenvalues at the points (24) are double and have a Jordan chain of generalized eigenvectors of order 2. In the complex plane the eigenvalues of the perturbed system move with the variation of Ω along the lines $\mathrm{Re}\,\lambda = -d_b$ until they meet at the points (24) and then split in the orthogonal direction; however, they never cross the imaginary axis, see Fig. 3(b).

The bubble of instability has two remarkable properties important for the explanation of the phenomenon of squeal. First, there exist perturbations causing its growth and emersion above the surface $\mathrm{Re}\,\lambda = 0$ (flutter); second, for small δ the instability is localized in the vicinity of the frequency $\mathrm{Im}\,\lambda = \beta$ and of the value of the gyroscopic parameter $\Omega = 0$. The bubble is a latent source of subcritical flutter instability localized in a narrow range of change of the gyroscopic parameter with $|\Omega| < \Omega_d$ at the frequency corresponding to the double eigenvalue of the non-rotating system.

Indefinite damping: An active state of the bubble of instability

As it is seen from equations (22), the radius of the bubble of instability is greater then the depth of its submersion under the surface $\mathrm{Re}\,\lambda = 0$ only if the eigenvalues μ_1 and μ_2 of the damping matrix have different signs, *i.e. if the damping is indefinite*. The damping with the indefinite matrix is a destabilizing factor [15, 44, 45]. It appears in the systems with frictional contact when the friction coefficient is decreasing with relative sliding velocity [14, 21, 23]. In our case it leads to the emersion of the bubble of instability so that the eigenvalues of the bubble have positive real parts in the range $\Omega^2 < \Omega_{cr}^2$, where the critical value is found from the equation (19)

$$(25)\quad \Omega_{cr} = \frac{\delta}{2}\sqrt{-\det\mathbf{D}}\,.$$

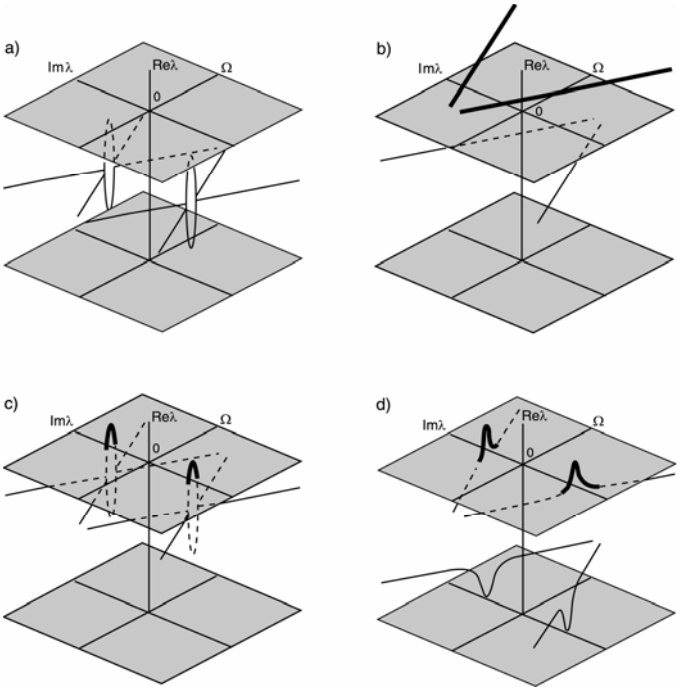

Figure 4. The mechanism of subcritical flutter instability (unstable eigenvalue branches are marked bold).

The right side of the formula (25) is real only for $\det \mathbf{D} < 0$, i.e. for the indefinite matrix $\mathbf{D}$. We see that in the plane of the parameters δ and Ω the domain of asymptotic stability is defined by the constraints $\delta \mathrm{Tr}\mathbf{D} > 0$ and $\Omega^2 > \Omega_{cr}^2$. For $\det \mathbf{D} < 0$ an unstable system with indefinite damping can be stabilized by sufficiently strong gyroscopic forces, as shown in Fig. 5(a) by the dashed line. With the increase in $\det \mathbf{D}$ the stability domain is getting wider and for $\det \mathbf{D} > 0$ it is defined by the condition $\delta \mathrm{Tr}\mathbf{D} > 0$, Fig. 5(c). At $\det \mathbf{D} = 0$ the line $\Omega = 0$ does not belong to the domain of asymptotic stability, Fig. 5(b). Therefore, changing the damping matrix $\delta\mathbf{D}$ from positive definite to indefinite one, we trigger the state of the bubble of instability from latent $\mathrm{Re}\,\lambda < 0$ to active $\mathrm{Re}\,\lambda > 0$, see Fig. 4(a,c). Since for small δ we have $\Omega_{cr} < \Omega_d$, the flutter instability is localized in the vicinity of $\Omega = 0$.

ACTIVATION OF THE BUBBLE OF INSTABILITY BY NON-CONSERVATIVE POSITIONAL FORCES

In the absence of dissipation non-conservative positional forces destroy the marginal stability of gyroscopic systems [5]. One can easily check that this property is valid for system (1) by assuming $\delta = \kappa = 0$ in the formulas (10) and (11), which yield

$$(26)\quad \lambda_p^{\pm} = i\beta \pm i\Omega \pm \frac{\nu}{2\beta}, \quad \lambda_n^{\pm} = -i\beta \pm i\Omega \mp \frac{\nu}{2\beta}.$$

The eigenvalues of the branches $i\beta + i\Omega$ and $-i\beta - i\Omega$ get positive real parts due to perturbation. The eigenvalues of the other two branches are shifted to the left from the imaginary axis, see Fig. 4(b). Thus, the instability induced by the non-conservative forces only is not localized near the nodes of the spectral mesh, in contrast to the effect of indefinite damping.

We show now that in combination with the dissipative forces, both definite and indefinite, the non-conservative forces can create subcritical flutter instability in the vicinity of the nodes of the spectral mesh. Multiplying equations (13), where we assume $\kappa = 0$, we find that the trajectories of the eigenvalues in the complex plane are described by the formula

$$(27)\quad \left(\mathrm{Re}\,\lambda + \frac{\mathrm{Tr}\mathbf{D}}{4}\delta\right)(\mathrm{Im}\,\lambda - \beta) = \frac{\Omega\nu}{2\beta}.$$

When $\nu = 0$ and $\delta \neq 0$ is given, the eigenvalues move with the variation of Ω along the lines $\mathrm{Re}\,\lambda = -\mathrm{Tr}\mathbf{D}/4$ and $\mathrm{Im}\,\lambda = \beta$ and merge at the points (24), see Fig. 3(b). Non-conservative positional forces with $\nu \neq 0$ destroy the merging of modes. As a consequence, the eigenvalues move along the separated trajectories. The eigenvalues with $|\mathrm{Im}\,\lambda|$ increasing due to an increase in $|\Omega|$ are closer to the imaginary axis then the others, as shown in Fig. 6(b). Therefore, in the space $(\Omega, \mathrm{Im}\,\lambda, \mathrm{Re}\,\lambda)$ the action of the non-conservative positional forces separates the bubble of instability and the adjacent hyperbolic eigenvalue branches into two non-intersecting curves, see Fig. 4(d).

The form of each of the new eigenvalue curves carries the memory about the original bubble of instability. As a consequence, the real parts of the eigenvalues are positive for the values of the gyroscopic parameter localized near $\Omega = 0$ in the range $\Omega^2 < \Omega_{cr}^2$. Taking into account that $\mathrm{Re}\,\lambda = 0$ at the critical values of the gyroscopic parameter we find Ω_{cr} from (13)

$$(28)\quad \Omega_{cr} = \delta\frac{\mathrm{Tr}\mathbf{D}}{4}\sqrt{-\frac{\nu^2 - \delta^2\beta^2 \det \mathbf{D}}{\nu^2 - \delta^2\beta^2(\mathrm{Tr}\mathbf{D}/2)^2}}.$$

Additionally, it follows from (13) that the eigenfrequencies of the unstable modes from the interval $\Omega^2 < \Omega_{cr}^2$ are localized near the frequency of the double semi-simple eigenvalue at the node of the undeformed spectral mesh: $\omega_{cr}^- < \omega < \omega_{cr}^+$, where

$$(29)\quad \omega_{cr}^{\pm} = \beta \pm \frac{\nu}{2\beta}\sqrt{-\frac{\nu^2 - \delta^2\beta^2 \det \mathbf{D}}{\nu^2 - \delta^2\beta^2(\mathrm{Tr}\mathbf{D}/2)^2}}.$$

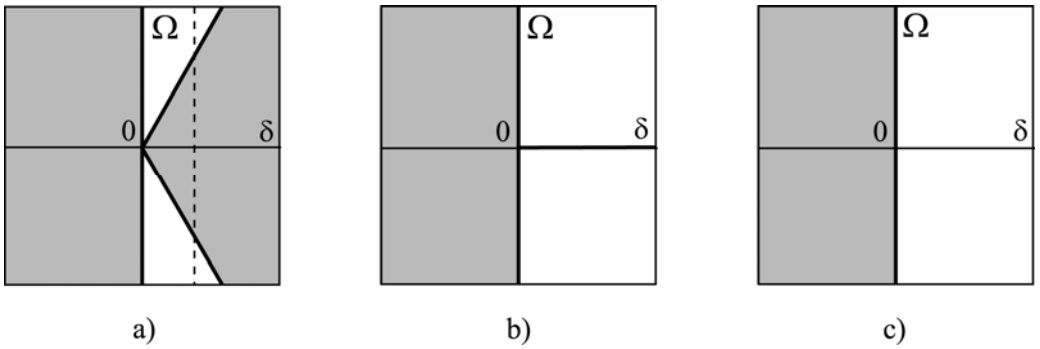

Figure 5.

Approximation to the domain of asymptotic stability (white) and its boundary (bold lines) for the dissipatively perturbed gyroscopic system (1) when: $\mathrm{Tr}\mathbf{D} > 0$ and $\det \mathbf{D} < 0$ (a); $\det \mathbf{D} = 0$ (b); $\det \mathbf{D} > 0$ (c).

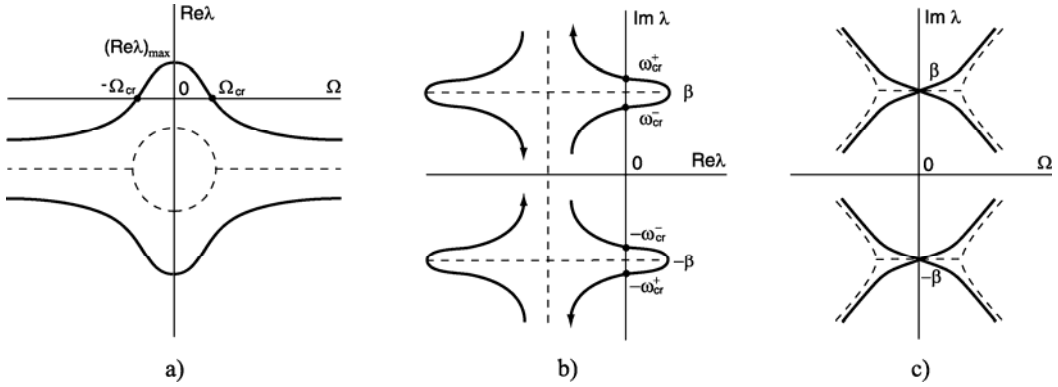

Figure 6. Subcritical flutter instability due to combined action of dissipative and non-conservative positional forces.

When the radicand in formulas (28) and (29) is real, the eigenvalues move in the complex plane making an excursion to its right side, as shown in Fig. 6(b). As it follows from (28), in presence of non-conservative positional forces such excursions behind the stability boundary are possible for the eigenvalues, even when dissipation is full: $\det \mathbf{D} > 0$. One can say that similarly to the indefinite damping *the non-conservative positional forces activate the latent sources of flutter instability created by the full dissipation*.

The equation (28) describes the surface in the space of the parameters δ, ν, and Ω, which is an approximation to the stability boundary separating the domains of asymptotic stability and flutter. For better understanding its shape we rewrite (28) in the form

$$\nu = \pm\delta\beta\,\mathrm{Tr}\mathbf{D}\sqrt{\frac{\delta^2 \det \mathbf{D} + 4\Omega^2}{\delta^2(\mathrm{Tr}\mathbf{D})^2 + 16\Omega^2}}. \quad (30)$$

If $\det \mathbf{D} \geq 0$ and Ω is fixed, (30) is an equation of two independent curves in the plane (δ, ν). The curves intersect with each other at the origin along the straight lines given by the expression $\nu = \pm\beta\,\mathrm{Tr}\mathbf{D}\delta/2$. However, in case when damping is indefinite and $\det \mathbf{D} < 0$, the radical in the formula (30) is real only for $\delta^2 < -4\Omega^2 / \det \mathbf{D}$. Then, (30) describes two branches of a closed loop in the plane of the parameters δ and ν. The loop is smooth at every point except at the origin, where it is self-intersecting with the tangents given by the expression $\nu = \pm\beta\,\mathrm{Tr}\mathbf{D}\delta/2$. Therefore, for a given Ω this curve looks like figure "8". When Ω goes to zero, the size of the self-intersecting curve tends to zero too. We conclude that in case $\det \mathbf{D} < 0$ the shape of the surface given by equation (28) or (30) is a cone with the "8"-shaped loop in a cross-section, see Fig. 7(a). Due to self-intersections the cone consists of four pockets. The asymptotic stability domain is inside the two of them, selected by the first inequality (23), as shown in Fig. 7(a). The singularity of the stability domain at the origin is the degeneration of a more general configuration described first in [45]. The domain of asymptotic stability bifurcates when $\det \mathbf{D}$ changes from negative to positive values. This process is shown in Fig. 7. According to (38) with increasing $\det \mathbf{D} < 0$ two pockets of the domain of asymptotic stability move towards each other until they have a common tangent line $\nu = 0$ at $\det \mathbf{D} = 0$, see Fig. 7(b).

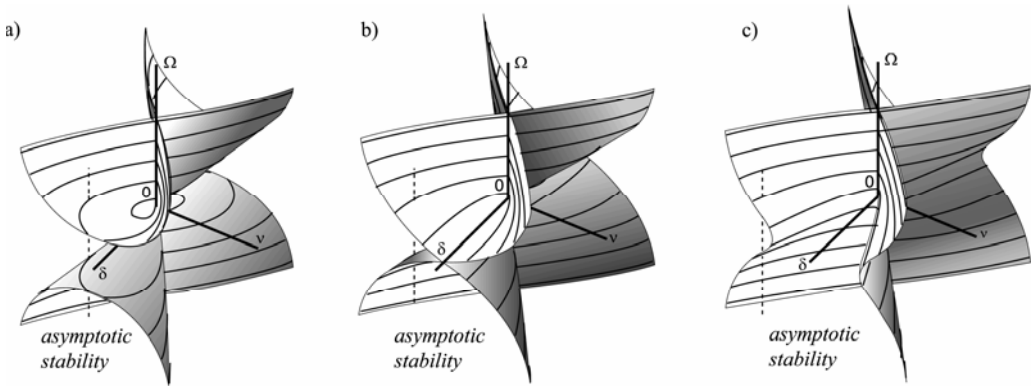

Figure 7.
Domains of asymptotic stability in the space (δ,ν,Ω) for different types of damping: Indefinite damping $\det\mathbf{D}<0$ (a); semi-definite (pervasive) damping $\det\mathbf{D}=0$ (b); full dissipation $\det\mathbf{D}>0$ (c).

When $\det\mathbf{D}>0$ this temporarily glued configuration unfolds to the unique domain of asymptotic stability bounded by the two surfaces intersecting along the Ω-axis, see Fig. 7(c).

In Fig. 7(a) we see that in case of indefinite damping there always exists an instability gap due to the singularity at the origin. Starting in the flutter domain at $\Omega=0$ for any combination of the parameters δ and ν one can reach the domain of asymptotic stability at higher values of $|\Omega|$ (gyroscopic stabilization), as shown in Fig. 7(a) by the dashed line. The gap is responsible for the subcritical flutter instability localized in the vicinity of the node of the spectral mesh of the unperturbed gyroscopic system. When $\det\mathbf{D}=0$, the gap vanishes in the direction $\nu=0$. In case of full dissipation ($\det\mathbf{D}>0$) the singularity at the origin unfolds. However, the memory about it is preserved in the two instability gaps located in the folds of the stability boundary with the locally strong curvature, Fig. 7(c). We see that in case of full dissipation for some combinations of the parameters δ and ν the system is asymptotically stable at any Ω. There exist, however, the values of δ and ν for which one can penetrate the fold of the stability boundary with the change of Ω, as shown in Fig. 7(c) by the dashed line. For such δ and ν the flutter instability is localized in the vicinity of $\Omega=0$. It is remarkable that in presence of non-conservative positional forces the system with full dissipation can suffer from the subcritical flutter localized near the nodes of the spectral mesh. A good illustration of this fact is the formula for the maximal real part of the unstable eigenvalue attained at $\Omega=0$ (see Fig. 6(a))

$$(31)\quad (\mathrm{Re}\,\lambda)_{\max}=-\frac{\mu_1+\mu_2}{4}\delta+\sqrt{\left(\frac{\mu_1-\mu_2}{4}\right)^2\delta^2+\frac{\nu^2}{4\beta^2}}.$$

From our previous considerations it follows that the phenomenon of the local subcritical flutter instability is controlled by the eigenvalues of the matrix $\mathbf{D}$. When both of them are positive, the folds of the stability boundary are more pronounced if one of the eigenvalues is close to zero. If one of the eigenvalues is negative and the other is positive, the local subcritical flutter instability is possible for any combination of δ and ν including the case when the non-conservative positional forces are absent ($\nu=0$).

Even if the structure of the damping matrix $\mathbf{D}$ is unknown, we realize that the main role of dissipation of any kind is the creation of the bubble of instability. The bubble is submerged below the surface $\mathrm{Re}\,\lambda=0$ in the space $(\Omega,\mathrm{Im}\,\lambda,\mathrm{Re}\,\lambda)$ in case of full dissipation and partially lies in the domain $\mathrm{Re}\,\lambda>0$ when damping is indefinite. Non-conservative positional forces split the bubble of instability into two branches and shift one of them to the region of positive real parts even in case of full dissipation. Since the branch remembers the existence of the bubble, the instability is developing locally near the nodes of the spectral mesh.

Therefore, the instability mechanism behind the squeal is the emersion (or activation) due to indefinite damping and non-conservative positional forces of the bubbles of instability created by the full dissipation in the vicinity of the nodes of the spectral mesh.

EXAMPLE. A ROTATING CIRCULAR STRING CONSTRAINED BY A STATIONARY LOAD SYSTEM

Consider a rotating circular string of displacement $W(\varphi,\tau)$, constrained at $\varphi=0$ by a spring, a damper, and a massless eyelet [13]. The eyelet generates a constant frictional follower force F [13, 16] on the string, as shown in Fig. 8. The parameters r and ρ are the radius and mass per unit length of the string.

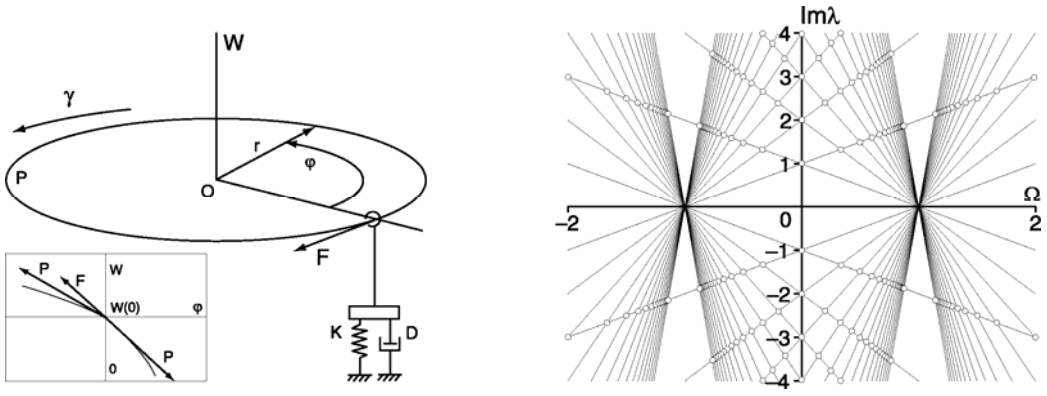

Figure 8.
A rotating circular string and its 'keyboard' constituted by the nodes of the spectral mesh (only 30 modes are shown).

The following assumptions are adopted in developing the governing equation of the problem: the circumferential tension P in the string is constant; the stiffness of the spring supporting the string is K and the damping coefficient of the viscous damper is D; the velocity of the string in the φ direction has constant value γr, where the rotational speed of the string is γ [13]. Introducing non-dimensional variables and parameters

$$t=\frac{\tau}{r}\sqrt{\frac{P}{\rho}},\quad w=\frac{W}{r},\quad \Omega=\gamma r\sqrt{\frac{\rho}{P}},$$
$$k=\frac{Kr}{P},\quad \mu=\frac{F}{P},\quad d=\frac{D}{\sqrt{\rho P}},\tag{32}$$

we arrive at the non-dimensional governing equation and boundary conditions [13]:

$$w_{tt}+2\Omega w_{t\varphi}-(1-\Omega^2)w_{\varphi\varphi}=0,\tag{33}$$

$$w(0,t)-w(2\pi,t)=0,$$
$$(1-\Omega^2)[w_{\varphi}(2\pi,t)-w_{\varphi}(0,t)]\tag{34}$$
$$+kw(0,t)+dw_t(0,t)+\mu w_{\varphi}(0,t)=0.$$

The boundary conditions (34) reflect the continuity of the string displacement and the discontinuity of its slope. They follow from the force balance at the eyelet in the assumption of smallness of the norm of w and $w(\varphi)$ with respect to r. The inclusion in Fig. 8 shows the mutual configuration of the vectors of the frictional follower force F and of the circumferential tension P.

Separation of time $w(\varphi,\mathrm{t})=u(\varphi,\mathrm{t})\exp(\lambda,\mathrm{t})$ yields the boundary eigenvalue problem

$$Lu=\lambda^2+2\Omega\lambda u'-(1-\Omega^2)u''=0,\tag{35}$$

$$u(0)-u(2\pi)=0,$$
$$u'(0)-u'(2\pi)=\frac{\lambda d+k}{1-\Omega^2}u(0)+\frac{\mu}{1-\Omega^2}u'(0),\tag{36}$$

where prime denotes partial differentiation with respect to φ. The non-self-adjoint boundary eigenvalue problem depends on four parameters Ω, d, k, and μ, expressing the speed of rotation, and damping, stiffness, and friction coefficients of the eyelet, respectively.

Taking the scalar product $(Lu,v)=\int_0^{2\pi}\bar{v}Lud\varphi$, where the bar over a symbol denotes complex conjugate, then integrating it by parts and employing the boundary conditions (36) we arrive at the boundary value problem adjoint to (35) and (36)

$$L^*v=\bar{\lambda}^2v-2\Omega\bar{\lambda}v'-(1-\Omega^2)v''=0,\tag{37}$$

$$v(0)-v(2\pi)=-\frac{\mu}{1-\Omega^2}v(2\pi),$$
$$v'(0)-v'(2\pi)=\frac{\bar{\lambda}d+k}{1-\Omega^2}v(2\pi)+\frac{2\Omega\mu}{(1-\Omega^2)^2}v(2\pi).\tag{38}$$

Let us first consider the string without constraints ($d=k=\mu=0$). Then, the system is gyroscopic so that the eigenfunctions of the adjoint boundary value problems corresponding to a purely imaginary eigenvalue λ coincide, i.e. $v=u$. Assuming the solution of the equation (35) in the form $u=C_1\exp(\varphi\lambda/(1-\Omega))+C_2\exp(-\varphi\lambda/(1+\Omega))$ and substituting it into the boundary conditions (36) we obtain the characteristic equation

$$8\lambda\sin\frac{\pi\lambda}{i(1-\Omega)}\sin\frac{\pi\lambda}{i(1+\Omega)}\frac{e^{\frac{-2\pi\lambda\Omega}{\Omega^2-1}}}{\Omega^2-1}=0,\tag{39}$$

The roots of the equation (39) are

$$\lambda_n^{\pm} = in(1 \pm \Omega), \tag{40}$$

where n is an integer. They are the eigenvalues of the problem (35), (36) with the eigenfunctions

$$u_n^{\pm} = \cos(n\varphi) \mp i \sin(n\varphi), \tag{41}$$

respectively. The eigenvalues are purely imaginary and form a mesh of lines intersecting with each other in the plane $\mathrm{Im}\,\lambda$ versus Ω, as shown in Fig. 8. Two eigenvalue branches $\lambda_n^{\varepsilon} = in(1 + \varepsilon\Omega)$ and $\lambda_m^{\delta} = im(1 + \delta\Omega)$, where $\varepsilon, \delta = \pm$, intersect each other at $\Omega = \Omega_{mn}^{\varepsilon\delta}$

$$\Omega_{nm}^{\varepsilon\delta} = \frac{n - m}{m\delta - n\varepsilon} \tag{42}$$

and originate the double eigenvalue

$$\lambda_{mn}^{\varepsilon\delta} = \frac{inm(\delta - \varepsilon)}{m\delta - n\varepsilon}, \tag{43}$$

which has two linearly independent eigenfunctions

$$\begin{aligned} u_n^{\varepsilon} &= \cos(n\varphi) - \varepsilon i \sin(n\varphi), \\ u_m^{\delta} &= \cos(m\varphi) - \delta i \sin(m\varphi). \end{aligned} \tag{44}$$

The nodes (42), (43) of the spectral mesh of the rotating circular string in the absence of the external loading are marked by white dots in Fig. 8. At $\Omega = 0$ the spectrum of the non-rotating string consists of the double semi-simple purely imaginary eigenvalues in, $n \in Z$. Each of them splits into two simple purely imaginary eigenvalues due to change in the angular velocity [7, 8, 13, 17]. At $\Omega = \pm 1$ all the eigenvalue branches cross the axis $\mathrm{Im}\,\lambda = 0$, see Fig. 8. In the following we will consider the spectrum for the angular velocities from the subcritical range $\Omega \in (-1,1)$.

Proceeding analogously to our investigation of a two-dimensional system we study the splitting of the double eigenvalues at the nodes of the spectral mesh caused by the interaction of the rotating string with the external loading system. For this purpose we use the perturbation theory of multiple eigenvalues of non-self-adjoint differential operators developed in [28, 33, 38]. According to this theory the perturbed eigenvalues are expressed by the following asymptotic formula

$$\begin{aligned} \lambda = \lambda_{nm}^{\varepsilon\delta} &- \frac{f_{nn}^{\varepsilon\varepsilon} + f_{mm}^{\delta\delta}}{2} - \frac{\xi_{nn}^{\varepsilon\varepsilon} + \xi_{mm}^{\delta\delta}}{2} \\ &\pm \sqrt{\frac{(f_{nn}^{\varepsilon\varepsilon} - f_{mm}^{\delta\delta} + \xi_{nn}^{\varepsilon\varepsilon} - \xi_{mm}^{\delta\delta})^2}{4} - (f_{nm}^{\varepsilon\delta} + \xi_{mn}^{\delta\varepsilon})(f_{nm}^{\varepsilon\delta} + \xi_{mn}^{\delta\varepsilon})}. \end{aligned} \tag{45}$$

The coefficients $f_{nm}^{\varepsilon\delta}$ are defined by

$$f_{nm}^{\varepsilon\delta} = \frac{\Delta\Omega}{N}\left(\lambda_{nm}^{\varepsilon\delta}\int_0^{2\pi} u_n'^{\varepsilon}\bar{u}_m^{\delta}\,d\varphi + \Omega_{nm}^{\varepsilon\delta}\int_0^{2\pi} u_n''^{\varepsilon}\bar{u}_m^{\delta}\,d\varphi\right), \tag{46}$$

$$N = \sqrt{\int_0^{2\pi}(\lambda_{nm}^{\varepsilon\delta}u_n^{\varepsilon} + \Omega_{nm}^{\varepsilon\delta}u_n'^{\varepsilon})\bar{u}_n^{\varepsilon}\,d\varphi\int_0^{2\pi}(\lambda_{nm}^{\varepsilon\delta}u_m^{\delta} + \Omega_{nm}^{\varepsilon\delta}u_m'^{\delta})\bar{u}_m^{\delta}\,d\varphi}$$

while the quantities $\xi_{nm}^{\varepsilon\delta}$ are

$$\xi_{nm}^{\varepsilon\delta} = \frac{1}{2N}\left((d\lambda_{nm}^{\varepsilon\delta} + k)u_n^{\varepsilon}(0)\bar{u}_m^{\delta}(0) + \mu u_n'^{\varepsilon}(0)\bar{u}_m^{\delta}(0)\right), \tag{47}$$

where $\Delta\Omega = \Omega - \Omega_{nm}^{\varepsilon\delta}$. Calculating the integrals and taking into account expressions (43) and (44), we obtain

$$\begin{aligned} \lambda = \lambda_{nm}^{\varepsilon\delta} &+ i\frac{\varepsilon n + \delta m}{2}\Delta\Omega + i\frac{n + m}{8\pi nm}(d\lambda_{nm}^{\varepsilon\delta} + k) \\ &+ \frac{\varepsilon + \delta}{8\pi}\mu \pm \sqrt{c}, \end{aligned} \tag{48}$$

$$\begin{aligned} c = &\left(i\frac{\varepsilon n - \delta m}{2}\Delta\Omega + i\frac{m - n}{8\pi mn}(d\lambda_{nm}^{\varepsilon\delta} + k) + \frac{\varepsilon - \delta}{8\pi}\mu\right)^2 \\ &- \frac{(d\lambda_{nm}^{\varepsilon\delta} + k - i\varepsilon n\mu)(d\lambda_{nm}^{\varepsilon\delta} + k - i\delta m\mu)}{16\pi^2 nm}. \end{aligned} \tag{49}$$

According to the experimental data the frequency of sound emitted by a singing wine glass and a squealing laboratory brake at low spins is close to a double eigenfrequency of the non-rotating bodies [19, 23, 34, 39, 40, 41]. For this reason we study first the influence of external stiffness, damping, and friction on the deformation of the spectral mesh near the nodes corresponding to $\Omega = 0$. Note, however, that the formulae (48) and (49) describe the deformation of the spectral mesh in the vicinity of arbitrary node.

Taking into account that $m = n$ and $\varepsilon = -\delta$ for the double eigenvalues $\lambda_{nm}^{\varepsilon\delta}$ at $\Omega = 0$, we find from (48) and (49) the expressions, describing splitting of the double eigenvalue in due to action of gyroscopic forces and an external spring

$$\lambda = in + i\frac{k}{4\pi n} \pm i\sqrt{n^2\Omega^2 + \frac{k^2}{16\pi^2 n^2}}. \tag{50}$$

The branches of the hyperbola (50) intersect the axis $\Omega = 0$ at the values $\lambda = n$ and $\lambda = n + k/(2\pi n)$ in the plane $\mathrm{Im}\,\lambda$ versus Ω, see Fig. 9(a). The gap between the branches decreases with the increase of the number n of a mode. The lower branch passes through the point corresponding to the node of the spectral mesh of the non-perturbed gyroscopic system, which agrees with the numerical results of [7, 13]. Remember that in case of two-dimensional systems the reason for such a degenerate behavior is a zero eigenvalue in the matrix $\mathbf{K}$ of external potential forces.

Analogously, from (48) and (49) the asymptotic formula follows describing the splitting of the double eigenvalue in at $\Omega = 0$ due to perturbation by the gyroscopic forces and an external damper

$$\lambda = in - \frac{d}{4\pi} \pm \sqrt{\frac{d^2}{16\pi^2} - n^2\Omega^2}. \quad (51)$$

The real parts of the eigenvalues as functions of Ω originate a bubble of instability in the plane $(\mathrm{Re}\,\lambda, \Omega)$

$$\left(\mathrm{Re}\,\lambda + \frac{d}{4\pi}\right)^2 + n^2\Omega^2 = \frac{d^2}{16\pi^2}, \quad \mathrm{Im}\,\lambda = n. \quad (52)$$

The ellipse (52) is submerged under the plane $\mathrm{Re}\,\lambda = 0$ in the space $(\Omega, \mathrm{Im}\,\lambda, \mathrm{Re}\,\lambda)$ so that it touches the plane at the origin, as shown in Fig. 9(b). The ellipse (52) is connected with the branches of the hyperbola of complex eigenvalues

$$n^2\Omega^2 - (\mathrm{Im}\,\lambda - n)^2 = \frac{d^2}{16\pi^2}, \quad \mathrm{Re}\,\lambda = -\frac{d}{4\pi}. \quad (53)$$

The external damper creates a latent source of local subcritical flutter instability exactly as it happens in two dimensions when the matrix of dissipative forces $\mathbf{D}$ is semi-definite, i.e. when it has one zero eigenvalue. The range of change of the gyroscopic parameter corresponding to the latent instability is located compactly around the origin and decreases with the increase in n.

The deformation of the spectral mesh near the double eigenvalue in at $\Omega = 0$ due to combined action of gyroscopic forces and external friction is described by the expression, following from (48) and (49)

$$\lambda = in \pm \sqrt{\left(in\Omega + \frac{\mu}{4\pi}\right)^2 - \frac{\mu^2}{16\pi^2}}. \quad (54)$$

The imaginary parts of the eigenvalues (54) are

$$\mathrm{Im}\,\lambda = n \pm \frac{1}{2\pi}\sqrt{2\pi^2 n^2\Omega^2 \pm \pi n\Omega\sqrt{4\pi^2 n^2\Omega^2 + \mu^2}}. \quad (55)$$

They cross at the node $(0, n)$, as in the non-perturbed case. However, the crossing is degenerate because the eigenvalue branches touch each other at the node, see Fig. 9(c). Expanding expression (55) in the vicinity of $\Omega = 0$ we find that

$$\mathrm{Im}\,\lambda = n \pm \frac{1}{2\pi}\sqrt{\pi n\mu\,|\,\Omega\,|} + O(\Omega^{3/2}). \quad (56)$$

Clearly, at $\Omega = 0$ the imaginary parts do not split due to non-conservative perturbation from the eyelet. For $\Omega \to \infty$ the imaginary parts asymptotically tend to $n(1 \pm \Omega)$. By this reason for small perturbations the spectral mesh in the plane $(\mathrm{Im}\,\lambda, \Omega)$ looks non-deformed at the first glance.

The real parts of the eigenvalues (55) are

$$\mathrm{Re}\,\lambda = \pm\frac{1}{2\pi}\sqrt{-2\pi^2 n^2\Omega^2 \pm \pi n\Omega\sqrt{4\pi^2 n^2\Omega^2 + \mu^2}}. \quad (57)$$

The crossing of the real parts at $\Omega = 0$ is degenerate Fig. 9(c), which is confirmed by the expression

$$\mathrm{Re}\,\lambda = \pm\frac{1}{2\pi}\sqrt{\pi n\mu\,|\,\Omega\,|} + O(\Omega^{3/2}). \quad (58)$$

For $\Omega \to \infty$ the real parts (57) follow the asymptotic law

$$\mathrm{Re}\,\lambda = \pm\frac{\mu}{4\pi} \mp \frac{\mu^3}{128\pi^3 n^2\Omega^2} + o(\Omega^{-2}). \quad (59)$$

As is also seen in Fig. 9(c), the real parts almost always are close to the lines $\pm\mu/(4\pi)$, except for the vicinity of the node of the spectral mesh, where the real parts rapidly tend to zero. This behavior agrees with the results of numerical calculations of [13]. We see that the double semi-simple eigenvalue in does not split due to variation of only the parameter of non-conservative positional forces μ. In the two-dimensional case this would correspond to the degenerate matrix $\mathbf{N}$, $\det\mathbf{N} = 0$. Since $\mathbf{N}$ is skew-symmetric, the degeneracy means $\mathbf{N} \equiv 0$, i.e. the absence of non-conservative perturbation. In case of more then two degrees of freedom the degeneracy of the operator of non-conservative positional forces leads to the cuspidal deviation of the generic splitting picture, see Fig. 9(c). Hence, the source of perturbation of the rotating string concentrated at one point leads to the deformation of its spectral mesh, which is similar to that caused by the semi-definite matrices of conservative, dissipative and non-conservative forces in the two-dimensional case.

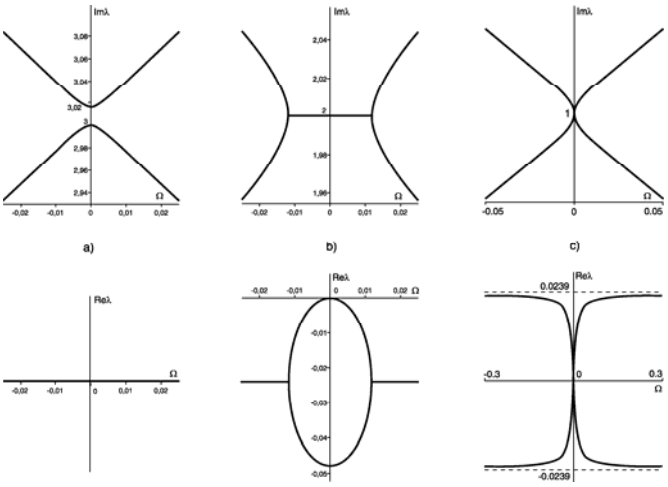

Figure 9. Deformation of the spectral mesh of the rotating string near the nodes (0,3), (0,2), and (0,1) caused by the action of the external spring with k=0.3 (a), a damper with d=0.3 (b), and friction with μ =0.3 (c).

Zero eigenvalues of the damping operator encourage the activation of the latent bubble of instability, while the zero eigenvalue of the operator of non-conservative positional forces suppresses this process. To get local subcritical flutter instability, described in the previous sections for the finite-dimensional model, the operators of dissipative and non-conservative perturbations must be generic, which excludes their semi-definiteness. One of the ways to avoid this degeneracy is to consider not pointwise [26] but distributed contact with the dissipative, stiffness, and friction characteristics depending on the material coordinates. A step in this direction is taken in [46], where a model of distributed pads was developed. For simplicity, in [46] the characteristics of the pins constituting the pads were assumed not depending on the coordinates, which caused the same semi-definite degeneracy. This could be a reflection of the so-called Herrmann-Smith paradox of a beam resting on a Winkler-type elastic foundation and loaded by a follower force [22]. The degeneracy in the Herrmann-Smith problem is removed by assuming a non-uniform modulus of elasticity. Similar modification of the model of the distributed brake pads could give generic perturbation operators so that the modeling of the disk brake squeal will catch its most significant features.

CONCLUSION: DISC BRAKE AS A MUSICAL INSTRUMENT

As we already mentioned, the principle of activating sound by friction is the same for a wine glass, a disc brake, and the glass harmonica. The latter is an ancient musical instrument for which the famous "Dance of the Sugar Plum Fairy" in the first edition of "The Nutcracker" ballet was composed by P.I. Tchaikowsky in 1891 [47].

The results obtained in the present paper show that the "keyboard" of the rotating elastic bodies of revolution, among which are the glass harmonica and the disc of a brake, is formed by the nodes of the spectral mesh, corresponding to angular velocities in the subcritical range. The frictional contact is the source of dissipative and non-conservative forces, which make the system unstable in the vicinity of the nodes and force a rotating structure to vibrate at a frequency close to the double frequency of the node and at the angular velocity close to that of the node. These conclusions agree with the results of recent experiments with the laboratory brake [39, 40, 41]. A particular frequency is selected by the speed of rotation and the loading conditions, including such parameters as the size of the friction pads and their placement with respect to the disc.

It is known that dissipative and non-conservative forces may influence the stability in a non-intuitive manner [5, 11, 25, 27, 36, 37, 45]. We have shown that the former create the latent local sources of instability around the nodes of the spectral mesh (bubbles of instability), while the latter activate these sources by inflating and destructing the bubbles. It turns out that the eigenvalues of the damping matrix control the development of instability. For better stability both of them should be positive and stay far from zero. If one of the eigenvalues of the damping matrix is close to zero or becomes negative, the instability can occur with the weaker non-conservative positional forces or even without them.

With the use of the perturbation theory of multiple eigenvalues we have obtained explicit formulas describing the deformation of the spectral mesh by dissipative and non-conservative perturbations. The trajectories of eigenvalues are analytically described and classified. The approximations of the domain of asymptotic stability are obtained with the use of the derivatives of the operator and the eigenvectors of the double eigenvalues calculated at the nodes of the spectral mesh. Singularities of the stability boundary of a new type were found and their role in the development of instability was clarified. The theory developed seems to be the first analytical description of the basic mechanism of friction-induced instabilities in rotating elastic bodies of revolution.

Comparing the generic results obtained in the two-dimensional case with that of the study of the rotating string we have shown that the widely employed concept of a point-wise contact leads to the semi-definite non-generic perturbation operators which suppress generic instability mechanism causing squeal. The further progress in the squeal simulation seems to significantly depend on creation of the models of distributed contact that do not allow for such a degeneration.

ACKNOWLEDGMENTS

The work has been supported by the Alexander von Humboldt Foundation and by the German Research Foundation, Grant DFG HA 1060/43-1.

REFERENCES

1. G. Bryan, On the beats in the vibrations of a revolving cylinder or bell. Proc. Cambridge Philos. Soc. 7, 101-111 (1890).
2. R. Southwell, On the Free Transverse Vibrations of a Uniform Circular Disc Clamped at its Centre; and on the Effect of Rotation. Proc. Roy. Soc. Lond. 101, 133–153 (1922).
3. W.D. Iwan, K.J. Stahl, The response of an elastic disc with a moving mass system. Trans. ASME. J. Appl. Mech. 40, 445-451 (1973).
4. A.W. Leissa, On a curve veering aberration. ZAMP 25, 99-111 (1974).
5. V.M. Lakhadanov, On stabilization of potential systems. Prikl. Mat. Mekh. 39(1), 53-58 (1975).
6. A.P. French, In Vino Veritas: A study of wineglass acoustics. Am. J. Phys. 51(8), 688-694 (1983).
7. G.S. Schajer, The vibration of a rotating circular string subject to a fixed end restraint. J. Sound Vibr. 92, 11-19 (1984).
8. N.C. Perkins, C.D. Mote, Comments on curve veering in eigenvalue problems. J. Sound Vibr. 106, 451-463 (1986).
9. S. Barnett, Leverrier's algorithm: a new proof and extensions. SIAM J. Matrix Anal. Appl. 10(4), 551-556 (1989).
10. K. Popp, P. Stelter, Stick-slip vibrations and chaos. Phil. Trans. R. Soc. Lond. A. 332, 89-105 (1990).
11. A.M. Bloch, P.S. Krishnaprasad, J.E. Marsden, T.S. Ratiu, Dissipation induced instabilities. Ann. Inst. H. Poincare. 11(1), 37-90 (1994).
12. T.D. Rossing, Acoustics of the glass harmonica. J. Acoust. Soc. Am. 95(2), 1106-1111 (1994).
13. L. Yang, S.G. Hutton, Interactions between an idealized rotating string and stationary constraints. J. Sound Vibr. 185(1), 139-154 (1995).
14. P. Freitas, M. Grinfeld, P.A. Knight, Stability of finite-dimensional systems with indefinite damping. Adv. Math. Sci. Appl. 7(1), 437-448 (1997).
15. W. Kliem, P.C. Mueller, Gyroscopic stabilization of indefinite damped systems. ZAMM 77(1), 163-164 (1997).
16. J.E. Mottershead, Vibration- and friction-induced instabilities in discs. Shock Vibr. Dig. 30(1), 14-31 (1998).
17. J. Tian, S.G. Hutton, On the mechanisms of vibrational instability in a constrained rotating string. J. Sound Vibr. 225(1), 111-126 (1999).
18. R. Hryniv, P. Lancaster, Stabilization of gyroscopic systems. ZAMM 81(10), 675-681 (2001).
19. A. Akay, Acoustics of friction. J. Acoust. Soc. Am. 111(4), 1525-1548 (2002).
20. O.N. Kirillov, A.P. Seyranian, Metamorphoses of characteristic curves in circulatory systems. J. Appl. Math. Mech. 66(3), 371-385 (2002).
21. K. Popp, M. Rudolph, M. Kroeger, M. Lindner, Mechanisms to generate and to avoid friction-induced vibrations. VDI-Berichte 1736, VDI-Verlag Duesseldorf, 1-15 (2002).
22. O.N. Kirillov, A.P. Seyranian, Solution to the Herrmann-Smith problem. Dokl. Phys. 47(10), 767-771 (2002).
23. N.M. Kinkaid, O.M. O'Reilly, P. Papadopoulos, Automotive disc brake squeal. J. Sound Vib.267, 105-166 (2003).
24. Y. Fukumoto, The three-dimensional instability of a strained vortex tube revisited. J. Fluid Mech.493, 287-318 (2003).
25. N. Hoffmann, L. Gaul, Effects of damping on mode-coupling instability in friction induced oscillations. ZAMM 83, 524-534 (2003).
26. O. M. O'Reilly, P. C. Varadi, On Some Peculiar Aspects of Axial Motions of Closed Loops of String in the Presence of a Singular Supply of Momentum, ASME J. Appl. Mech. 71(4), 541-545 (2004).
27. N.M. Bou-Rabee, J.E. Marsden, L.A. Romero, Tippe Top inversion as a dissipation-induced instability. SIAM J. Appl. Dyn. Sys. 3, 352-377 (2004).
28. O.N. Kirillov, A.P. Seyranian, Collapse of the Keldysh chains and stability of continuous non-conservative systems. SIAM J. Appl. Math. 64(4), 1383-1407 (2004).
29. S. Serafin, The sound of friction: real-time models, playability and musical applications. PhD Thesis. Stanford University, 1-224 (2004).
30. P. Hader, Selbsterregte Schwingungen von Papierkalandern. Shaker Verlag, Aachen 2005.
31. S. Vidoli, F. Vestroni, Veering phenomena in systems with gyroscopic coupling. Trans. ASME, J. Appl. Mech. 72, 641-647 (2005).
32. O.N. Kirillov, A.A. Mailybaev, A.P. Seyranian, Unfolding of eigenvalue surfaces near a diabolic point due to a complex perturbation. J. Phys. A: Math. Gen. 38(24), 5531-5546 (2005).
33. O.N. Kirillov, A.O. Seyranian, The effect of small internal and external damping on the stability of distributed non-conservative systems. J. Appl. Math. Mech. 69(4), 529-552 (2005).
34. H. Ouyang, W. Nack, Y. Yuan, F. Chen, Numerical analysis of automotive disc brake squeal: a review. Int. J. Veh. Noise and Vibr., 1(3/4), 207–231 (2005).
35. G. Jundt, A. Radu, E. Fort, J. Duda, H. Vach, Vibrational modes of partly filled wine glasses. J. Acoust. Soc. Am. 119(6), 3793-3798 (2006).
36. R. Krechetnikov and J.E. Marsden, On destabilizing effects of two fundamental non-conservative forces. Phys. D 214, 25-32 (2006).
37. O.N. Kirillov, Gyroscopic stabilization of non-conservative systems. Phys. Lett. A 359(3), 204-210 (2006).
38. U. Guenther, O.N. Kirillov, A Krein space related perturbation theory for MHD α^2-dynamos and resonant unfolding of diabolical points. J. Phys. A: Math. Gen. 39(32), 10057-10076 (2006).
39. F. Massi, O. Giannini, L. Baillet, Brake squeal as dynamic instability: an experimental investigation. J. Acoust. Soc. Am. 120(3), 1388-1398 (2006).

40. O. Giannini, A. Akay, F. Massi, Experimental analysis of brake squeal noise on a laboratory brake setup. J. Sound Vibr. 292, 1-20 (2006).
41. O. Giannini, A. Sestieri, Predictive model of squeal noise occurring on a laboratory brake. J. Sound Vibr. 296, 583-601 (2006).
42. T. Butlin, J. Woodhouse, Studies of the Sensitivity of Brake Squeal. Appl. Mech. and Mater. 5-6, 473-479 (2006).
43. U. von Wagner, D. Hochlenert, P. Hagedorn, Minimal models for disk brake squeal. J. Sound Vibr. 302(3), 527-539 (2007).
44. A.N. Kounadis, Flutter instability and other singularity phenomena in symmetric systems via combination of mass distribution and weak damping. Int. J. of Non-Lin. Mech. 42(1), 24-35 (2007).
45. O.N. Kirillov, Destabilization paradox due to breaking the Hamiltonian and reversible symmetry. Int. J. of Non-Lin. Mech. 42(1), 71-87 (2007).
46. G. Spelsberg-Korspeter, D. Hochlenert, O.N. Kirillov, P. Hagedorn, In- and out-of-plane vibrations of a rotating plate with frictional contact: Investigations on squeal phenomena. Trans. ASME, J. Appl. Mech. (2007) (submitted).
47. W. Zeitler, Tchaikowsky composes "Dance of the Sugar Plum Fairy" for the Glass Armonica. http://www.glassarmonica.com/armonica/history/composers/tchaikowsky.php (1994-2007).
48. J.-J. Sinou, L. Jezequel. Mode coupling instability in friction-induced vibrations and its dependency on system parameters including damping. Eur. J. Mech. A. 26, 106-122 (2007).
49. J.C. Huang, C. M. Krousgrill, A. K. Bajaj. An efficient approach to estimate critical value of friction coefficient in brake squeal analysis. Trans. ASME. J. Appl. Mech. 74(3), 534-541 (2007).

CONTACT

E-mail: kirillov@imec.msu.ru
kirillov@dyn.tu-darmstadt.de

Web address: http://onkirillov.narod.ru
http://www.dyn.tu-darmstadt.de/members/kirillov/